01 Aug 2010

A New Methodology for Hydrodynamic Similarity in Bubble Columns

Ashfaq Shaikh

Muthanna H. Al-Dahhan
Missouri University of Science and Technology, aldahhanm@mst.edu

A New Methodology for Hydrodynamic Similarity in Bubble Columns

Ashfaq Shaikh[1] and Muthanna Al-Dahhan[2]*

1. *Intermediates and Polyester Technology Division, Eastman Chemical Company, Kingsport, Tennessee, 37662*
2. *Missouri University of Science and Technology, Rolla, Missouri 65409*

A new hypothesis has been proposed in this work for hydrodynamic similarity that can be subsequently used for scale-up of bubble column reactors. The proposed hypothesis takes into account both global (by matching overall gas holdup) as well as local hydrodynamics (by matching time-averaged radial profile/cross-sectional distribution of gas holdup) to maintain similarity in two systems. The evaluation of proposed hypothesis has been accomplished utilising advanced diagnostic techniques such as gamma-ray computed tomography (CT) and computer automated radioactive particle tracking (CARPT). In this work, we experimentally demonstrate that similarity based only on global hydrodynamics does not necessarily ensure similar mixing and turbulence in two systems. It is essential to maintain similar global as well as local hydrodynamics. The hydrodynamic similarity that can be obtained by matching the commonly used dimensionless groups was also evaluated at these experimental conditions.

Une nouvelle hypothèse a été proposée dans ce travail pour une similitude hydrodynamique qui peut être utilisée ultérieurement pour la mise à l'échelle des réacteurs à colonnes à bulles. L'hypothèse proposée prend en compte à la fois l'hydrodynamique globale (en harmonisant le volume mort général) et locale (en harmonisant le profil radial à moyenne temporelle/la distribution transversale du volume mort) pour maintenir la similitude dans deux systèmes. L'évaluation de l'hypothèse proposée a été accomplie en utilisant des techniques diagnostiques avancées comme la tomographie par ordinateur à rayons gamma et le traçage des particules radioactives assisté par ordinateur (CARPT). Dans ce travail, nous démontrons expérimentalement que la similitude fondée uniquement sur l'hydrodynamique globale n'assure pas nécessairement un mélange et une turbulence semblables dans deux systèmes. Il est essential de maintenir une hydrodynamique globale et locale semblable. La similitude hydrodynamique que l'on peut obtenir en harmonisant les groupes adimensionnels couramment utilisés a également été évaluée à ces conditions expérimentales.

Keywords: reactor design and operation, multi-phase systems < fluid mechanics, turbulence < fluid mechanics, alternative energy resources < energy, oil, gas and coal < energy

INTRODUCTION

Bubble columns are two-phase gas–liquid systems in which a gas is dispersed through a sparger and bubbles through a liquid in vertical cylindrical columns, with or without internals. Sometimes suspended solids can be present in liquid, forming a slurry phase. Accordingly, it can be called as two-phase or three-phase bubble column. The liquid/slurry phase flow can be either cocurrent, counter-current or in batch mode with respect to the gas flow. The size of the solid particles ranges from 5 to 150 μm and solids loading up to 50% volume (Krishna et al., 1997). Generally, the operating superficial liquid velocity (in the range of 0–2 cm/s) has an order of magnitude smaller than the superficial gas velocity (1–50 cm/s). Hence, the hydrodynamics of such reactors are controlled mainly by the gas flow. Mainly two flow regimes exist in these reactors separated by a transition regime. The presence of these flow regimes is dependent upon various operating and design parameters. These flow regimes exhibit vastly different hydrodynamic behaviour and hence mixing and heat and mass transfer (Fan, 1989; Shaikh and Al-Dahhan, 2007).

Bubble columns offer numerous advantages such as simple construction, good heat, and mass transfer, no moving parts and thus

This work was performed as a part of doctoral thesis at Washington University in St. Louis, MO.
*Author to whom correspondence may be addressed.
E-mail address: aldahhanm@mst.edu
Can. J. Chem. Eng. 88:503–517, 2010

DOI 10.1002/cjce.20357
Published online in Wiley InterScience
(www.interscience.wiley.com)

reduced wear and tear, low operating and maintenance costs. One of the main disadvantages of bubble column reactors is significant back-mixing which can affect product conversion. The excessive back-mixing can be overcome by modifying the design of bubble column reactors such as the addition of internals, baffles, or introducing sieve plates. These reactors are widely used in chemical, petrochemical, and biochemical industries for various processes such as alkylation, oxidation, chlorination, wet oxidation of effluents, coal hydrogenation, polymerization of olefins (Fan, 1989). An important emerging application of these reactors is to convert syngas into liquid hydrocarbons, that is, Fischer–Tropsch (FT) synthesis. The combination of increase in demand for oil and energy sources and depleting oil reserves in the world demand development of alternative energy resources. In this context, there is a renewed interest in FT synthesis, which converts syngas [a mixture of CO and H_2 obtained either from natural gas (GTL) or coal (CTL) or biomass (BTL)] into liquid hydrocarbons in the range of gasoline and diesel. The profitability of FT synthesis depends on the market oil prices. To be economically viable and independent of market oil prices, capital expenditure (CAPEX) of such process needs to be equal to or below \$20 000 Barrels/day of installment cost. A multipronged approach, which consists of improved catalyst selectivity and efficiency in FT synthesis and economies of scale in larger reactor sizes, is needed to achieve this goal. The economies of scale demands reduced risk in scale-up to build large diameter reactors, which in turn necessitates reliable similarity criteria.

Although bubble columns are relatively simple in mechanical construction, the task of extrapolating small diameter behaviour to larger ones is always challenging and difficult. The key to such extrapolation is the proper understanding of its complex hydrodynamic behaviour because the dispersion and interfacial heat and mass transfer fluxes which often limit the chemical reaction rates are closely related to fluid dynamics of the system through gas–liquid contact area and the turbulence properties of the flow. In literature there have been considerable efforts towards developing similarity hypotheses. Shaikh (2007) reviewed these procedures in detail. However, for sake of brevity, a brief outline of reported scale-up methodologies has been presented in Table 1.

It is clear from Table 1 that scale-up procedures reported so far utilised the similarity of global parameters, such as overall gas holdup, for hydrodynamic similarity in two columns. Such similarity based on global parameters is not surprising, because over the years bubble column hydrodynamics have been quantified mostly by global parameters such as overall gas holdup and

Table 1. Summary of reported scale-up methodologies

Refs.	Proposed criteria
Wilkinson et al. (1992)	The gas holdup is virtually independent of the column dimensions and the sparger layout (for low as well as high pressures) provided following criteria are fulfilled: the column diameter has to be larger than 15 cm; the column height to diameter ratio has to be in excess of 5; the hole diameter of the sparger has to be larger than 1–2 mm. A correlation was proposed for overall gas holdup for scale-up purposes
Degaleesan (1997)	Any gas–liquid/slurry would exhibit the similar hydrodynamic behaviour as air–water system if both the systems have the same overall gas holdup. It was suggested that hydrodynamics and mixing at the equivalent superficial gas velocity, u_{Ge} in an atmospheric air–water system that results in the same overall gas holdups would represent the hydrodynamics and mixing in scaled up hot unit
Inga and Morsi (1997)	Extrapolating the results of laboratory scale stirred tank reactor to design industrial scale slurry bubble column based on similarity of the relative importance of mass transfer resistance in the overall reaction resistances, defined in terms of a dimensionless parameter, β_i which represents the balance between $k_L a$ (mass transfer coefficient) and k_0 (rate of consumption, pseudo kinetic constant for first order). Accordingly, maintaining the same β in two reactors will result in the same reactant concentration and catalyst activity and thereby the conversion and selectivity in two reactors
Fan et al. (1999)	Similar overall gas holdup provides similar hydrodynamics. Using the vast range of data collected from literature and their own data, an empirical correlation was proposed to estimate the gas holdup in terms of the following three dimensionless numbers, Mo_{SL}; (ρ_G/ρ_L); $[u_G^4\rho_G/(\sigma_L g)]$. It was suggested that maintaining these dimensionless groups the same in two systems would lead to similar overall gas holdup and hence mixing and hydrodynamics. This approach is similar to Degaleesan (1997)
Safoniuk et al. (1999) and Macchi et al. (2001)	They presented a scale-up method for three phase fluidized beds with the aid of the Buckingham pi theorem, which yielded five dimensionless numbers that have a profound effect on overall gas holdup. These dimensionless groups are Morton number, *Mo*; Etovos number, *Eo*; Reynolds number, *Re*; Density ratio; Superficial gas and liquid velocity ratio. Later, Macchi et al. (2001) have tested the scaling approach of Safoniuk et al. (1999) in three phase fluidized beds where the liquid phase was an aqueous solution of glycerol (a liquid mixture) in one column and silicone oil (a pure liquid) in the other. It was observed that, whenever five dimensionless numbers were the same in these systems, the overall gas holdups were within 11% of root mean standard deviations. However, the pressure fluctuations studies revealed that the power spectra in the two systems are different indicating a mismatch behaviour. Macchi et al. (2001) concluded that matching these five dimensionless numbers is inadequate to ensure hydrodynamic similarity
Krishna et al. (2001)	They proposed a strategy for scaling laboratory reactors to commercial ones based on Computational Fluid Dynamics (CFD) and developed correlations of various hydrodynamic parameters
van Baten et al. (2003)	They proposed a modified strategy for the use of CFD approach to scale up bubble column reactors. The drag coefficient and bubble diameter were calculated utilising only overall gas holdup data in small diameter column (5.1 cm). However, the validation of CFD simulation results with experiments in large diameter columns was not established
Zhang and Zhao (2006)	They proposed a strategy that tied flow behaviour and catalysis studies with that of process engineering which involved studying hydrodynamics in cold flow units, catalyst performance evaluation in an autoclave, and process investigation in pilot-scale continuous slurry bubble column reactor. However, neither any guidelines were provided regarding hydrodynamic similarity in cold and hot unit nor any results with successful scale-up were shown

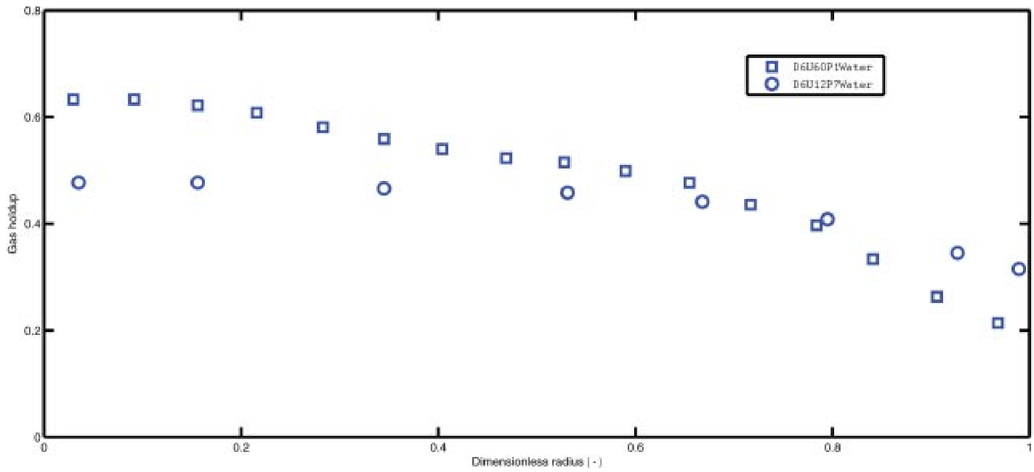

Figure 1. Comparison of gas holdup radial profile in a 0.162 m column using an air–water system at two different operating conditions (D6U12P7Water: 0.7 MPa, 0.12 m/s, an air–water Kemoun et al., 2001; D6U60P1Water: 0.1 MPa, 0.6 m/s, and an air–water Ong, 2003) with similar overall gas holdups (~0.41).

mass transfer coefficient. While hydrodynamic similarity based on overall hydrodynamics may be applicable in bubbly flow, which is characterised by uniform gas holdup radial profile and non-interacting bubbles; in the churn-turbulent flow regime, such criteria may possibly lead to a different gas holdup distribution across the column cross-section.

Figure 1 shows the gas holdup radial profile obtained using computed tomography (CT) in an air–water system (Kemoun et al., 2001; Ong, 2003) at different operating conditions in churn-turbulent flow regime with the overall gas holdup of 0.41. Although these systems have similar overall gas holdups, they have different gas holdup radial profiles that will clearly lead to different flow patterns and mixing intensities. One should note here that flow pattern has been described in terms of radial distribution of liquid axial velocity. The axial flow in bubble columns is much stronger than radial and azimuthal one and hence, liquid axial velocity was chosen. Mixing intensity is defined in terms of turbulent kinetic energy (TKE) which accounts for trace of a turbulence stress tensor. The conclusions of Macchi et al. (2001) and Figure 1 suggests that the two systems can have similar overall gas holdups but different flow patterns and mixing intensities. This indicates that two systems can be globally similar in nature, but have different local hydrodynamics. Hence, similarity based only on overall gas holdup does not appear sufficient.

Based on this, we propose a new methodology based on the hypothesis that:

"Overall gas holdup and its time-averaged radial profile or cross-sectional distribution should be the same for two reactors to be dynamically similar."

This work attempts to evaluate the proposed hypothesis utilising advanced diagnostic techniques such as CT and computer automated radioactive particle tracking (CARPT). Based on the combination of similarity and mismatch experiments, we will show whether similar overall gas holdups and similar gas holdup radial profiles reflect similar detailed local hydrodynamic performance in two reactors.

EXPERIMENTAL SETUP AND TECHNIQUES

The experiments were performed in a stainless steel column with an inner diameter of 0.162 m and a height of 2.5 m. High-pressure stainless steel column used in these experiments has been shown in Figure 2. The column is designed to support a maximum operating pressure of 1.15 MPa. The air as the gas phase was supplied from two compressors connected in parallel, with a working pressure of 1.45 MPa and a maximum corresponding rated flow of 8.8 m^3/min. The compressed atmospheric air was purified by passing it through a dryer and several air filter units. The air flow rate was controlled by a pressure regulator and rotameter setup, which consisted of four rotameters of increasing range connected in parallel. Air exited the column through a demister, passed through a back pressure regulator that controlled column operating pressure, and vented to the atmosphere. The column design enables easy removal of the distributor chamber and replacement of the sparger. Dried air at various pressures was the gas phase, while water (viscosity, $\mu_L = 1.0$ cP; density, $\rho_L = 998\ kg\,m^{-3}$; surface tension, $\sigma_L = 72\ dyn\,cm^{-1}$) and mixture of C9–C11 (viscosity, $\mu_L = 1.16$ cP; density, $\rho_L = 724\ kg\,m^{-3}$; surface tension, $\sigma_L = 24.8\ dyn\,cm^{-1}$) were the liquid phase.

Single Source γ-Ray Computed Tomography (CT)

CT has been extensively implemented on various multiphase flow systems at the Chemical Reaction Engineering Laboratory (CREL), Washington University. Software and hardware details of the single source γ-ray CT have been explained elsewhere in detail (Kumar, 1994). The CT setup consists of an array of detectors with an opposing source, which rotate together around the object to be scanned. The scanner uses a Cesium (Cs-137) encapsulated γ-ray source with activity of ~85 mCi. The array of detectors and the source are mounted on a gantry which can be rotated 360° around the object to be scanned, using a step motor. Also, the source–detector setup can be moved up and down to scan cross-sections at any axial position of the column. In the present study, 5 NaI scintillation detectors were used. Each detector consists of a cylindrical 0.0508 m × 0.0508 m NaI crystal, a photo multiplicator (PM), and electronics, forming a 0.054 m × 0.26 m cylindrical assembly. In each view, every detector acquires seven projections covering the total angular span of 2.72° of the detector face. A total of 99 views were acquired, with 3.6° of angular shift after every view. Hence, 3645 (5 × 7 × 9) projections were used to reconstruct the phase holdup distribution at each cross-sectional plane. The entire system is completely automated to acquire the data needed

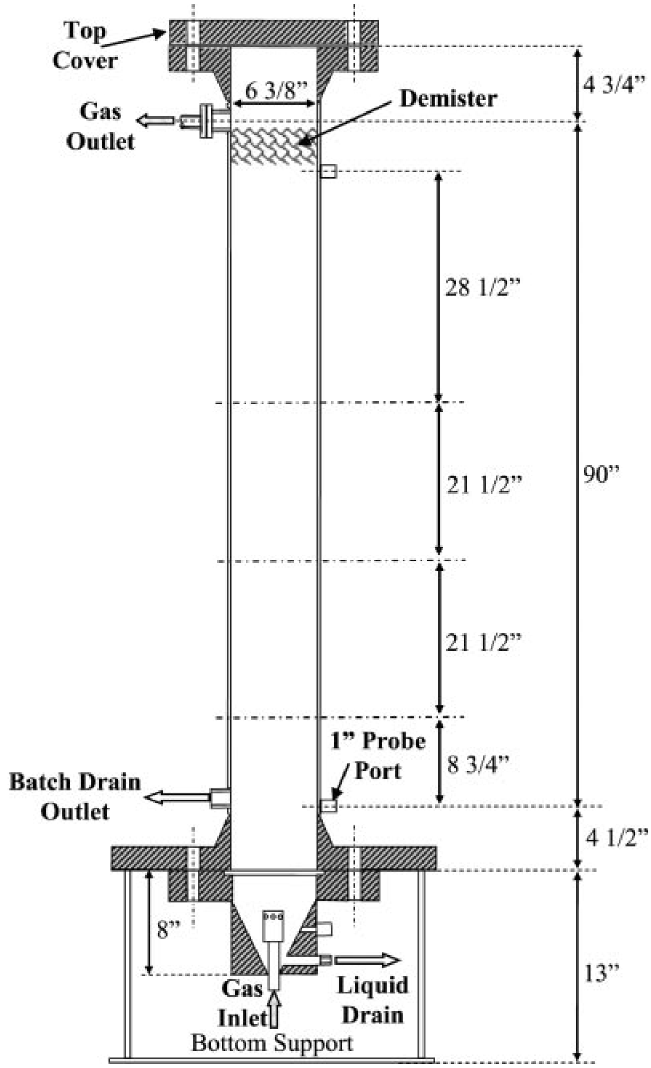

Figure 2. Bubble column reactor of 0.162 m diameter used for CARPT/CT measurements.

for the reconstruction of the phase distribution in a given cross-section. The estimation-maximisation (EM) algorithm has been used for image reconstruction (Kumar, 1994). It is based on maximum likelihood principles and takes into account the stochastic nature of the γ-ray beam projection measurements.

According to Beer–Lambert's law, for a single γ radiation source, absorbance A over the path l is equal to:

$$A = -\ln \frac{I}{I_0} = \sum_{l} (\rho\ \mu)_{ij} l_{ij} \tag{1}$$

where I_0 is the intensity of radiation emitted by the source, and I is the intensity of radiation received by the detector. Σ indicates the summation of the volumetric attenuation coefficient $(\rho\mu)_{ij}$ of each cell ij multiplied by the path length in that cell l_{ij} along the path l which the radiation beam traverses on its way from the source to the detector.

To obtain the holdup distribution, CT scans of the following systems need to be acquired: (1) an empty column ($K = \text{G}$), (2) a column filled with liquid ($K = \text{L}$), and (3) a column in operation with gas–liquid ($K = \text{GL}$). CT scans of actual experimental conditions as well as base scans were obtained using the same column, and hence the effect of wall is thus eliminated. In general, I_0 is unknown, and because of that the intensity of radiation I_K needs to be normalised with the intensity of radiation detected in the column containing only the gas phase I_{G}. Such normalisation yield the following equation for A_K:

$$A_K = -\ln \frac{I_K}{I_{\text{G}}} = \sum_{l} \left[(\rho\ \mu)_{K,ij} - (\rho\ \mu)_{\text{G},ij} \right] l_{ij} \tag{2}$$

For further simplification, a relative volumetric attenuation is defined as:

$$R_{K,ij} = (\rho\ \mu)_{K,ij} - (\rho\ \mu)_{\text{G},ij} \tag{3}$$

The volumetric attenuation coefficient for a gas–liquid system is:

$$(\rho\ \mu)_{\text{GL},ij} = (\rho\ \mu)_{\text{G},ij} \varepsilon_{\text{G},ij} + (\rho\ \mu)_{\text{L},ij} (1 - \varepsilon_{\text{G},ij}) \tag{4}$$

Using EM algorithm, $(\rho\ \mu)_{K,ij}$ (where $K = \text{G}$, L, and GL) will be estimated and hence $R_{K,ij}$ can be obtained. Therefore, from Equations (3) and (4), gas holdup in each pixel can be calculated as:

$$\varepsilon_{\text{G},ij} = 1 - \left(\frac{R_{\text{GL},ij}}{R_{\text{L},ij}} \right) \tag{5}$$

Computer Automated Radioactive Particle Tracking (CARPT)

CARPT technique involves tracking the temporal Lagrangian trajectories of a radiotracer (Sc46) particle (density = 2.5 g cc^{-1}) with the aid of a strategically located array of scintillation detectors. A calibration map of detector counts versus particle distance has to be obtained first in order to evaluate the instantaneous tracer locations and subsequently the liquid recirculation velocity and turbulence parameters. This was done by placing a radioactive particle at several known locations (~2000–3000 locations) in the system operated at a condition of interest. For this purpose, a new automated calibration device developed by Rados (2003) has been utilised. To track the liquid phase, the effective density of radioactive particle was matched with that of the density of liquid phase. This was accomplished by placing irradiated 150 μm Sc46 particle in 0.8 mm polypropylene particle and adjust the air gap to achieve composite particle density close to the density of the liquid to be traced. At all operating conditions a total of 30 scintillation detectors were positioned between $z/D = 1.9$ and 8.7. Thus, a calibration map (counts vs. distance) is obtained. The particle is then introduced into the column at the desired operating conditions and the experiment is conducted for 24 h at acquisition frequency of 50 Hz. With this data set and the calibration map information, the instantaneous positions of the particle were obtained using the improved reconstruction algorithm developed by Rados (2003). The time differentiation of the displacement yields local velocities. The ensemble averaged velocity profiles and "turbulent" parameters can then be computed with the aid of improved algorithm proposed by Rados (2003).

Essentially, CT provides cross-sectional distribution of phase holdups and CARPT provides instantaneous liquid velocity and its radial profile as well as turbulent parameters profile. In this study, for better understanding we will present time- and azimuthally averaged gas holdup and axial liquid velocity radial profiles.

EXPERIMENTAL CONDITIONS

The first step in the experimental evaluation of the proposed hypothesis to develop a new scale-up methodology was to identify the needed operating conditions. The experimental conditions were identified that have the same overall gas holdup and gas holdup radial profile. These conditions are called similarity conditions. Additionally, experimental conditions were identified such that it has the same overall gas holdup, but mismatched gas holdup radial profiles. These conditions are called as mismatch conditions. The provision to identify mismatch conditions is to further demonstrate that similarity of gas holdup and its radial profile is essential to maintain similar hydrodynamic performance.

The procedure for experimental evaluation of the proposed methodology is as follows:

(1) Identify experimental conditions that have similar overall gas holdup. The overall gas holdup is obtained by measuring the change in liquid height [$\varepsilon_G = H_d - H_S/H_d$] (where H_d and H_S are the dynamic and static liquid heights, respectively). In all these experiments, the dynamic height was kept around 1.8 m (L/D ∼ 11).
(2) Perform CT experiments at the conditions that have similar overall gas holdup to identify the conditions (i.e., superficial gas velocity, pressure, physical properties of the system) at which the same radial profile can be obtained. These conditions are called as similarity conditions.
(3) Perform CT experiments at the conditions that have similar overall gas holdup to identify the conditions (i.e., superficial gas velocity, pressure, physical properties of the system) at which the same overall gas holdup but mismatched gas holdup radial profiles can be obtained. These conditions are called as mismatch conditions.
(4) Perform CARPT experiments at the identified similarity/mismatch conditions to measure the detailed local hydrodynamics (radial profile of liquid velocity and turbulent parameters) in order to assess the methodology for attaining the hydrodynamic similarity as per the proposed hypothesis.

Table 2 shows the similarity conditions (i.e., S1–S3), while Table 3 shows the mismatch conditions (M1–M2) identified during this study. The gas holdup radial profiles at the conditions of similar overall gas holdup have been measured using CT at the desired conditions. A few experimental conditions in this study are extracted from the CREL database (references mentioned in Tables 2 and 3), in addition to the performed experiments. Although CT and CARPT experiments in an air–water system were performed earlier in the CREL, most of these experiments were repeated in this study. Unless it is referenced, the experiments were performed as a part of this work.

Table 2. Similarity conditions in a 0.162 m diameter stainless steel column

Set	System	Pressure (MPa)	Superficial gas velocity (cm/s)	Overall gas holdup
S1	Air–water	0.1	45	0.35
	Air–water	0.4	30	
S2	Air–water	1.0	30	0.41
	Air–water (Ong, 2003)	0.4	45	
S3	Air–water	0.4	30	0.35
	Air–C9–C11 (Han, 2006)	0.1	30	

Table 3. Experimental conditions for mismatch gas holdup radial profiles in a 0.162 m diameter stainless steel column.

Set	System	Pressure (MPa)	Superficial gas velocity (cm/s)	Overall gas holdup
M1	Air–water	0.4	30	0.35
	Air–C9–C11	0.4	16	
M2	Air–water	0.4	30	0.35
	Air–C9–C11	1.0	8	

The emphasis here is to show that if one maintains similar overall gas holdup and gas holdup radial profile, the hydrodynamic characteristics of these two systems will be the same. Such a hydrodynamic similarity is the ultimate goal of any scale-up procedure to maintain the desired conversion and process performance.

RESULTS

The gas holdup radial profiles, axial liquid velocity profiles, and TKE radial profiles shown in this section are time- and azimuthally averaged. The statistical difference between hydrodynamic parameter (gas holdup and liquid axial velocity) profiles are represented in terms of the average absolute relative difference (AARD) and absolute relative difference (ARD) and is defined as follows:

$$\mathrm{AARD} = \frac{1}{N}\sum_{1}^{N}\left|\frac{x(r) - y(r)}{x(r)}\right|, \quad (6a)$$

$$\mathrm{ARD} = \left|\frac{x(r) - y(r)}{x(r)}\right|, \quad (6b)$$

where x and y can either be gas holdup, axial liquid velocity, or TKE at the corresponding radial location for the similarity/mismatch cases to be assessed.

The strength of liquid recirculation at similarity/mismatch conditions is described in terms of mean liquid recirculation velocity. The liquid recirculation velocity is defined as:

$$\overline{u_{\mathrm{rec}}} = \frac{\int_0^{\eta^*} u_z(\eta)[1 - \varepsilon_G(\eta)]\eta d\eta}{\int_0^{\eta^*} [1 - \varepsilon_G(\eta)]\eta d\eta}, \quad (7)$$

where η^* is the radial position of flow inversion.

Similarity Conditions

S1 set of conditions

Figure 3a shows the gas holdup radial profiles at experimental conditions of 45 cm/s, and 0.4 MPa (Ong, 2003), and 30 cm/s and 1 MPa in an air–water system. The gas holdup radial profiles are close to each other, with an AARD of 5.5%. The similar gas holdup radial profiles in these cases result in close liquid axial velocity profiles (Figure 3b) with an AARD of 14%. Figure 4 shows the variation of an ARD at these conditions. Except at the inversion point, an ARD appears to be close to 10%. The relatively higher AARD can be attributed to such a large difference at the inversion point.

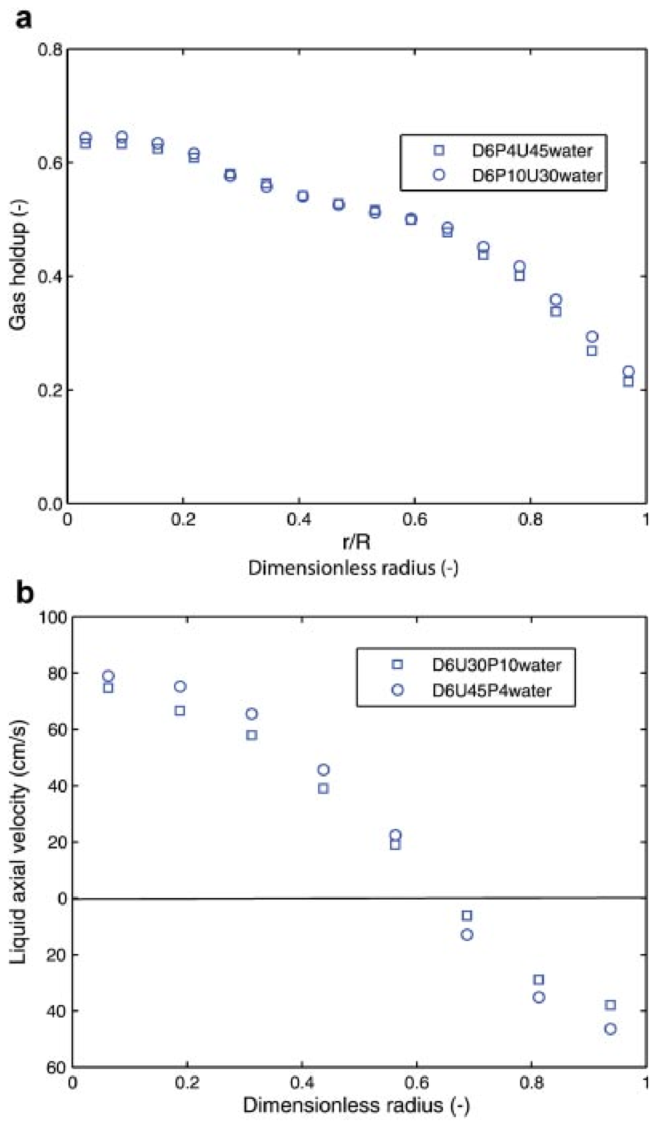

Figure 3. (a) Gas holdup and (b) axial liquid velocity radial profile in a 0.162 m diameter stainless steel column using an air–water system (D6P4U45: 6 in. diameter, 0.4 MPa, and 45 cm/s Ong, 2003, D6P10U30: 6 in. diameter, 1 MPa, and 30 cm/s) (overall gas holdup ~0.41).

At all the studied conditions, an ARD was found to be maximum close to the inversion point. A possible reason is that the values of the velocities are low (i.e., −6 and −13 cm/s) in this region (sometimes one condition has a positive value, and other has a negative value) and the relative differences between these values gets amplified and subsequently increases the AARD.

Additionally, mean liquid recirculation was calculated at these conditions using Equation (7). The mean recirculation velocity at 30 cm and 1 MPa is 52 cm/s, while at 45 cm/s and 0.4 MPa, it is 55 cm/s. The relative difference between mean recirculation velocities at these conditions is 5.5%. The mixing intensity at these conditions is expressed in terms of the TKE of the system at those conditions. Figure 5 compares the radial distribution of TKE at these similarity conditions. The AARD in TKE at these conditions was found to be close to 11%. This shows that the similar gas holdup radial profiles resulted in close axial velocity and TKE radial profiles, and thereby the close recirculation rates and mixing intensities.

S2 set of conditions

Figure 6a shows gas radial profiles at operating conditions of 30 cm/s and 0.4 MPa and 45 cm/s and 0.1 MPa in an air–water system. The overall gas holdup in these cases is 0.35. The AARD in gas holdup radial profiles was found to be 4.5%. Such close gas radial profiles result in close liquid axial velocity profiles (Figure 6b). The AARD in liquid axial velocity profiles is 17%. The variation of ARD along the column radius is shown in Figure 7. In this case also, the ARD appears to be higher near the inversion point, as explained above. The mean recirculation velocity at 30 cm/s and 0.4 MPa is 42 cm/s, while at 45 cm/s and 0.1 MPa, it is 39.5 cm/s. The relative difference between mean recirculation velocities is close to 6%, indicating similar liquid recirculation patterns and its strength at these conditions. Figure 8 shows a comparison between TKE at these conditions. The AARD in TKE was found to be within 9%, indicating similar mixing intensity and liquid recirculation at these conditions.

S3 set of conditions

Figure 9a shows the gas holdup radial profiles at 30 cm/s and 0.1 MPa in an air–C9C11 system (Han, 2007) and 30 cm/s and 0.4 MPa in an air–water system. In this set of experiments, one experimental condition uses a pure liquid (water), while the other uses a mixture of *n*-paraffins. The mix-

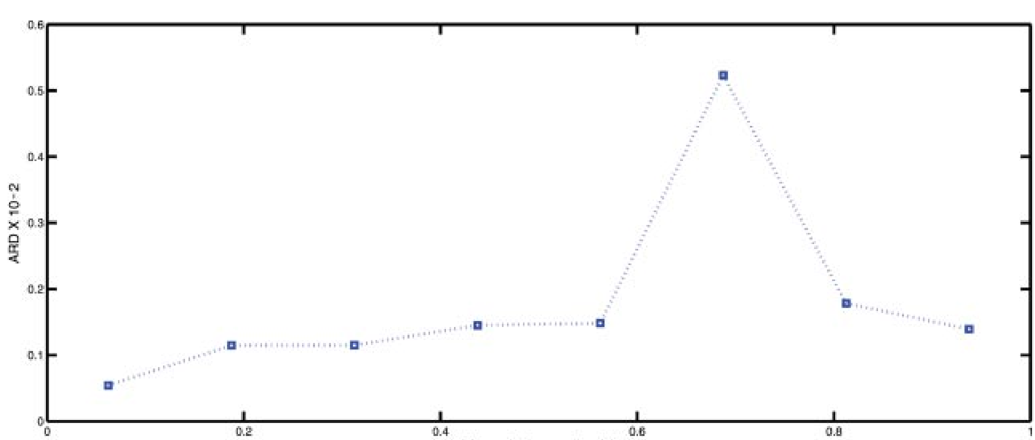

Figure 4. Variation of ARD in liquid axial velocities between similarity conditions (D6P4U45Water Ong, 2003 and D6P10U30Water) along the column radius in a 0.162 m diameter stainless steel column using an air–water system.

ture of paraffinic liquid is predominantly C9–C11 cut. The compositions of the various *n*-paraffins are ≤C8 3.3%, C9 36.3%, C10 34.5%, C11 23.8%, and ≥C12 1.9%. The physical properties of this mixture are also vastly different from water (density = 0.726 g cc^{-1}; viscosity = 0.85 mPa s; surface tension = 23.2 mN m^{-1}). The experiments with such different liquids were motivated by the findings of Macchi et al. (2001) who used one system with a pure liquid and another with a mixture of liquids. They found that although the overall gas holdup in these two systems matched within allowable statistical difference (11%), the power spectra in these systems were different. Thus, even though the systems were globally similar, their local behaviour differed. The current work sought to evaluate whether maintaining the hypothesis proposed in this work would provide similar hydrodynamic performance, even if one system had a pure liquid and the other one had a mixture of liquids.

Figure 9a shows close gas holdup radial profiles in this case, except close to the centre of the column. An AARD in gas holdup radial profiles is within 4%. Figure 9b shows the liquid axial velocities in these cases. An AARD in the liquid axial velocity profile was found to be close, within 14%. As in other cases, the maximum ARD (120%) was found at the inversion point (Figure 10). The values of the velocities at this point are 0.93 and −3.85 cm/s.

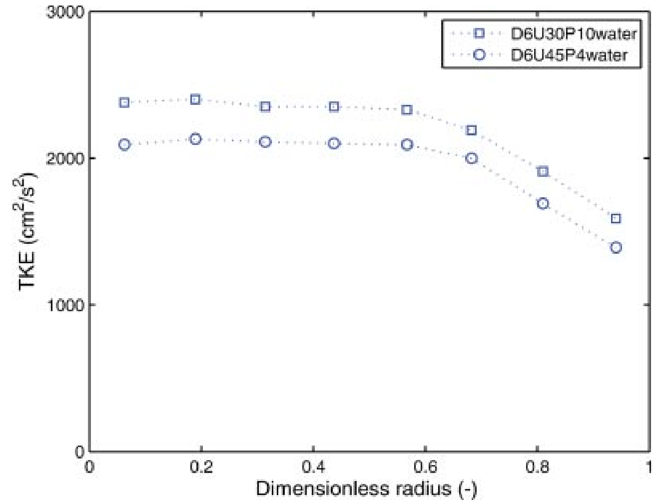

Figure 5. TKE profile in a 0.162 m diameter stainless steel column using an air–water system (D6P4U45: 6 in. diameter column, 0.4 MPa and 45 cm/s Ong, 2003, D6P10U30: 6 in. diameter column, 1 MPa and 30 cm/s) (overall gas holdup ~0.41).

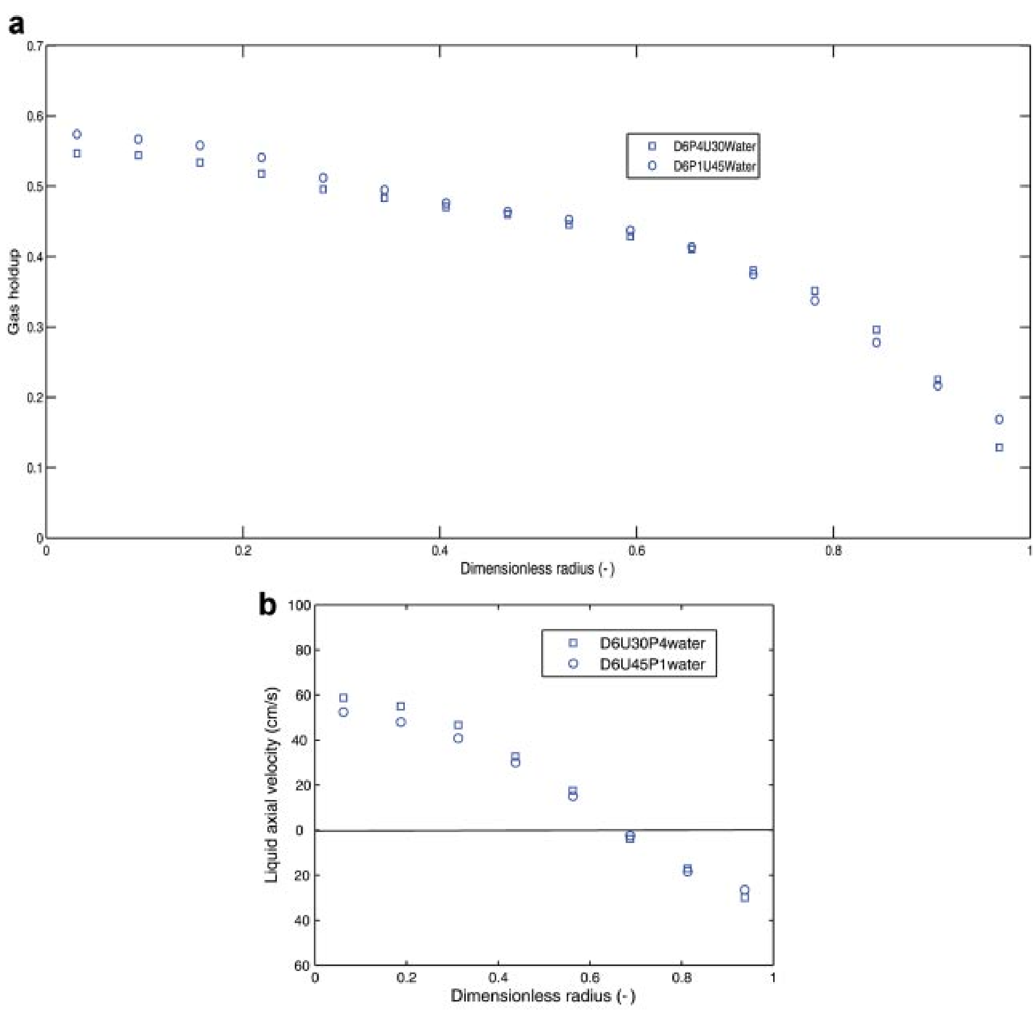

Figure 6. (a) Gas holdup and (b) axial liquid velocity radial profile in a 0.162 m diameter stainless steel column using an air–water system (D6P1U45Water: 6 in. diameter column, 0.1 MPa, and 45 cm/s, D6P4U30Water: 6 in. diameter column, 0.4 MPa, and 30 cm/s) (overall gas holdup ~0.35).

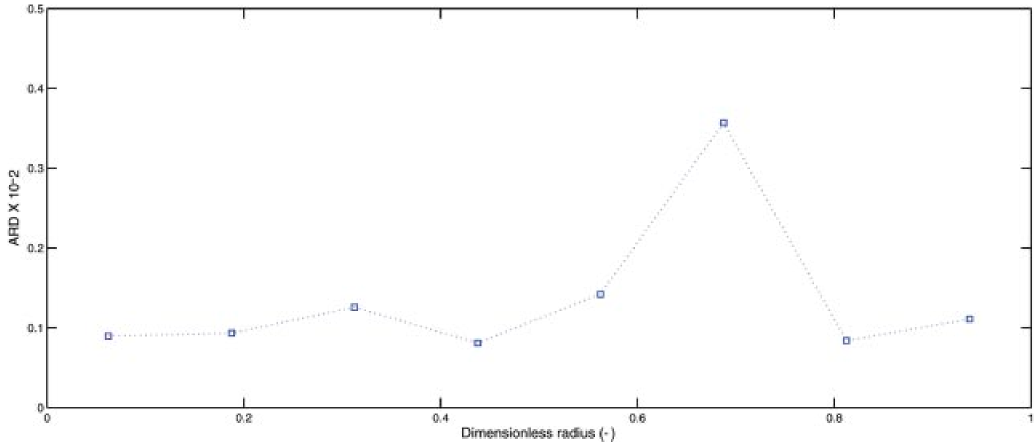

Figure 7. Variation of ARD in liquid axial velocities between similarity conditions (D6P1U45water and D6P4U30water) along the column radius in a 0.162 m diameter stainless steel column using an air–water system.

The positive and negative values of liquid velocity led to a higher ARD at the inversion point as mentioned earlier. The mean liquid recirculation velocity in an air–water system was 42 cm/s, while in an air–C9C11 system it was 41 cm/s. The relative difference of mean recirculation velocities in this set is 3%, indicating similar strength of liquid recirculation in these systems. Figure 11 shows the radial profile of TKE with an AARD of 8.5%, reflecting similar distributions of TKE at these conditions that indicate a similar mixing intensity in these systems.

Based on set S3, we have demonstrated that maintaining the hypothesis proposed in the current work results in similar liquid recirculation and mixing intensity, even if one system has pure liquid and other one has a mixture of liquids. It shows that bulk liquid physical properties are sufficient to describe the liquid phase only when the gas holdup radial profiles are matched in two systems.

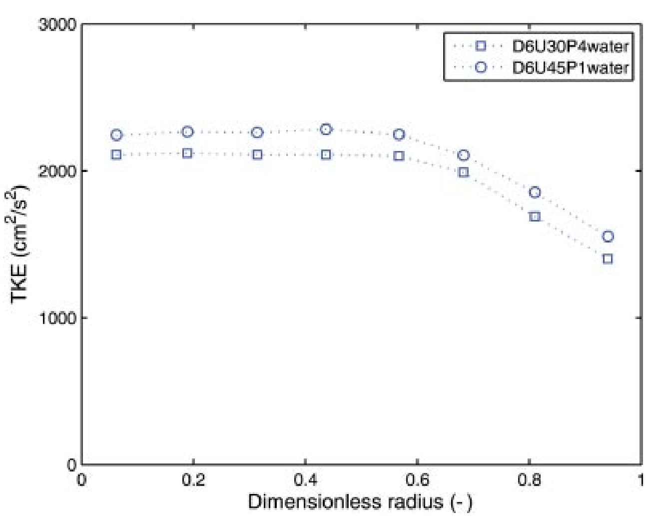

Figure 8. TKE radial profile in a 0.162 m diameter stainless steel column using an air–water system (D6P1U45Water: 6 in. diameter column, 0.1 MPa, and 45 cm/s, D6P4U30Water: 6 in. diameter column, 0.4 MPa, and 30 cm/s) (overall gas holdup ~0.35).

Mismatch Conditions

M1 set of conditions

Figure 12a shows a set of experimental conditions where the overall gas holdup is the same, that is, 0.35. Although the overall gas holdup is the same, the gas holdup radial profiles in these cases are mismatched. AARD, of gas holdup radial profile between 30 cm/s and 0.4 MPa in an air–water system and 16 cm/s and 0.4 MPa in an air–C9C11 system, is 13%. The mismatched gas holdup radial profiles result in different liquid axial velocities (Figure 12b). An AARD in liquid axial velocities is 35%. Figure 13 shows that, similar to earlier sets of experiments, the maximum ARD is near the inversion point ($r/R = 0.8$); moreover, the ARD in axial velocities at the remaining radial locations was consistently above 20%. The mean recirculation velocity at 30 cm/s and 0.4 MPa in an air–water system was 42 cm/s, while at 16 cm/s and 0.4 MPa, it was 30 cm/s. The relative difference between mean liquid recirculation velocities was 28%. The radial profile of TKE at these conditions was compared to evaluate how the mismatched gas holdup radial profiles affect mixing intensity. Although the qualitative distribution of TKE appears to be similar at these conditions, there exists a significant quantitative difference in their magnitudes. An AARD in the radial profile of TKE was found to be around 27%, as shown in Figure 14. It is obvious that as the differences increase between the gas holdup radial profiles, the differences between the detailed local hydrodynamics also increase.

M2 set of conditions

Figure 15 shows set M2 of mismatch experimental conditions (30 cm/s and 0.4 MPa in an air–water system, and 8 cm/s and 1 MPa in an air–C9C11 system). The overall gas holdup at these conditions is also the same 0.35; however, an AARD in gas holdup radial profiles is 25%. The mismatched radial profiles result in entirely different liquid recirculation velocities, with an AARD in velocities close to 48%. In this case also, the ARD of liquid axial velocities (Figure 16) is consistently above 40%. The mean recirculation velocity at 30 cm/s and 0.4 MPa in an air–water system is 42 cm/s, while at 8 cm/s and 1 MPa, it is 22 cm/s. The relative

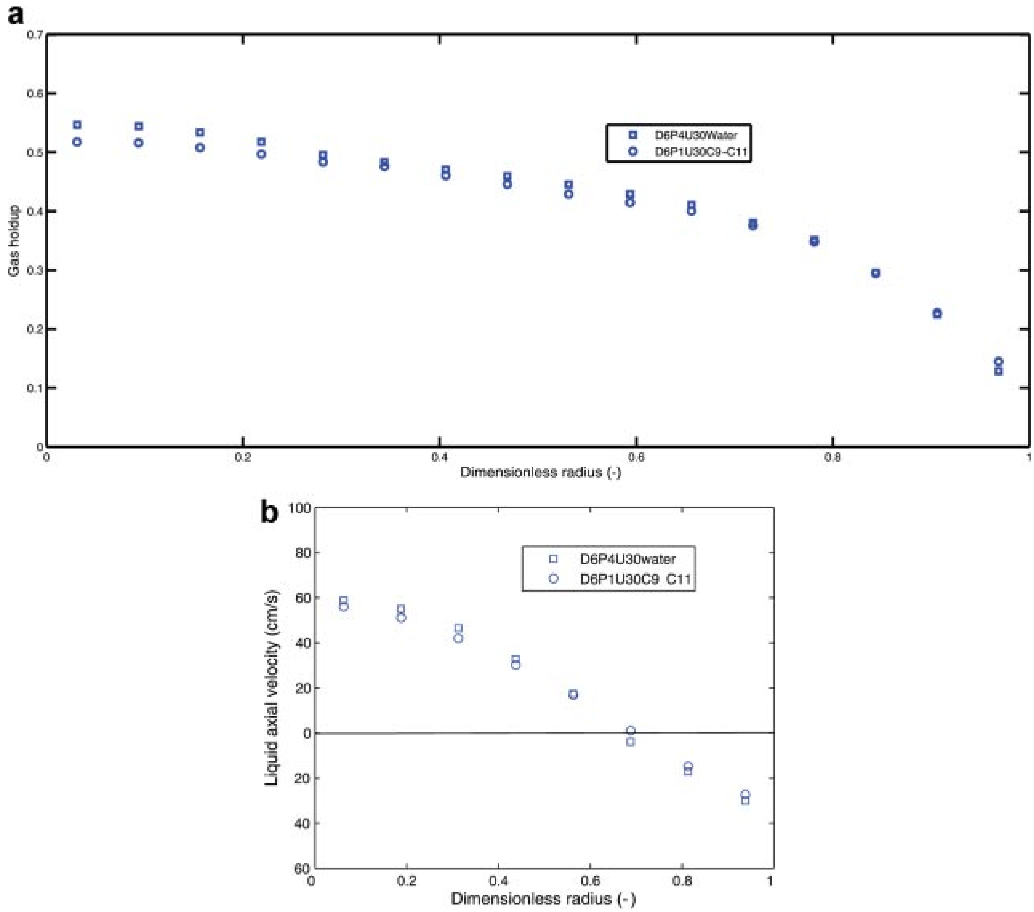

Figure 9. (a) Gas holdup and (b) axial liquid velocity radial profile in a 0.162 m diameter stainless steel column (D6P1U30 C9–C11: 6 in. diameter column, 0.1 MPa, 30 cm/s Han, 2007, and air–C9–C11 fluid system, D6P4U30water: 6 in. diameter column, 0.4 MPa, 30 cm/s, and an air–water system) (overall gas holdup ~0.35).

difference between mean liquid recirculation velocities is 47%. Figure 17 shows the radial distribution of TKE at these conditions. An AARD in the radial profile of TKE is around 45%. One should note here that in this case there exist both qualitative and quantitative differences in TKE. The distribution of TKE at 8 cm/s and 10 bars appears to be uniform, possibly because of the relatively uniform gas holdup radial profile. Again, as the differences increase between the gas holdup radial profiles, the differences between the detailed local hydrodynamics also increase.

DISCUSSION

Based on the sets of mismatch experiments, two points are worth mentioning:

(a) The radial or cross-sectional distribution of gas holdup indicates that one set of mismatch experiments, M2 has one condition (30 cm/s, 0.4 MPa, an air–water) operating in the churn-turbulent flow regime, while the other condition (8 cm/s, 1 MPa, air–C9–C11) appears close to bubbly or tran-

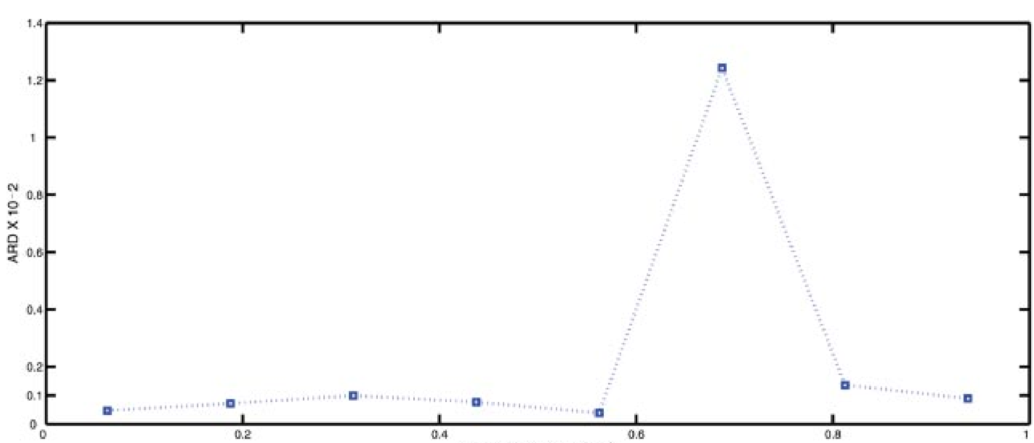

Figure 10. Variation of ARD in liquid axial velocities between similarity conditions (D6P1U30 C9–C11 Han, 2007 and D6P4U30water) along the column radius in a 0.162 m diameter stainless steel column.

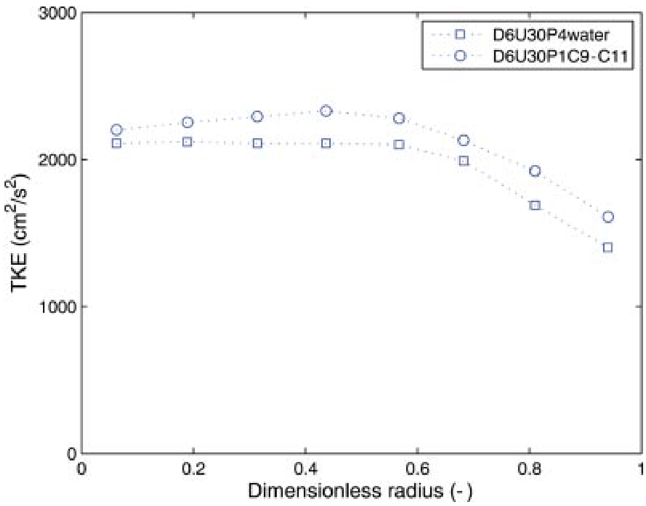

Figure 11. TKE radial profile in a 0.162 m diameter stainless steel column (D6P1U30 C9–C11: 6 in. diameter column, 0.1 MPa, 30 cm/s, and air–C9–C11 fluid system, D6P4U30water: 6 in. diameter column, 0.4 MPa, 30 cm/s, and an air–water system) (overall gas holdup ~0.35).

sition flow although they have similar overall gas holdups. It shows that to be hydrodynamically similar it is *necessary* that both the systems, apart from having similar global hydrodynamics, should operate in the same flow regime. Operation in the same flow regime ensures that bubble interaction and dynamics in these systems are similar.

(b) It is clear from the radial or cross-sectional distribution of gas holdup in the first set of mismatch experiments, M1 that both the systems operate in the churn-turbulent flow regime. However, due to mismatched gas holdup radial profiles, these systems show different liquid recirculations and mixing intensities. Hence the combination of two sets of mismatch experiments shows that the condition that two systems must operate in the same flow regime to be hydrodynamically similar is *necessary* but not *sufficient*. It shows the importance of matching gas holdup radial profiles or cross-sectional distributions in two systems, even if both systems operate in the same flow regime.

The current work combines the set of similarity and mismatch experiments and demonstrates that to be hydrodynamically similar, it is necessary to have similarity of both overall gas holdup and gas holdup radial profile. The similarity conditions showed that similar overall gas holdup and gas holdup radial profiles resulted in close liquid recirculation and mixing intensity in both systems. The mismatch experiments had similar overall gas holdups but mismatched profiles, and resulted in varied liquid recirculation and mixing intensity. This clearly shows that maintaining similar overall gas holdup alone can lead to different recirculation and mixing, if gas holdup radial profiles are not matched. In addition, it can also be observed that increased AARD in gas holdup radial profiles results in even more increase in differences in local hydrodynamics.

Although overall gas holdup determines the magnitude of macroscopic hydrodynamics, the microscopic flow dynamics is controlled by gas phase motion due to the gradient of buoyancy forces between the column centre and the wall region. In churn-turbulent flow regime, there exists an unequal distribution of gas holdup along the column cross-section, with higher gas holdup in the centre and lower holdup in the wall region. A similarity based solely on overall gas holdup masks such distribution and lumps it into one global parameter. This simplistic approach lead to different mixing and flow patterns, as the momentum transferred by the gas phase motion is responsible for the liquid recirculation in such flows.

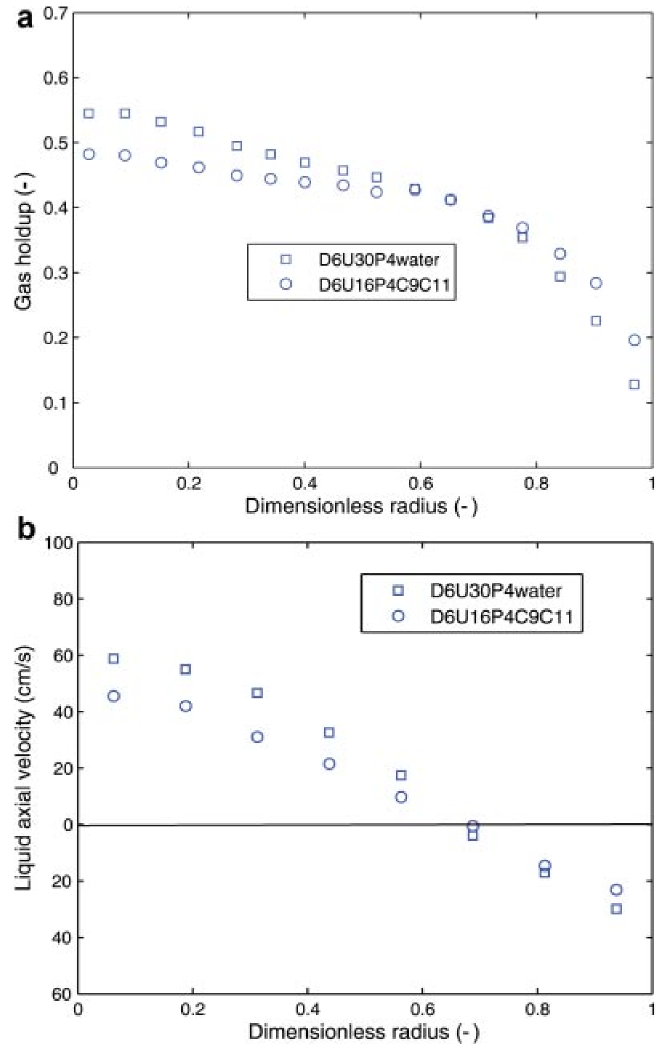

Figure 12. (a) Gas holdup and (b) axial liquid velocity radial profile in a 0.162 m diameter stainless steel column (D6P4U30water: 6 in. diameter column, 0.4 MPa, and 30 cm/s, an air–water; D6P4U16 C9–C11: 6 in. diameter column, 0.4 MPa, and 16 cm/s, air–C9–C11) (overall gas holdup ~0.35).

In bubbly flow, however, the distribution of bubble size is narrow and uniform along the column cross-section, resulting in relatively flat gas holdup radial profiles. Due to the absence of non-uniform microscopic flow behaviour; the determining factor in bubbly flow is the magnitude of the macroscopic hydrodynamics. Hence, the similarity of global parameters can be specifically applicable if both the systems operate in bubbly flow, and it may result in similar liquid recirculation and mixing intensity. To corroborate this fact, experiments with different operating conditions with the same overall gas holdup in bubbly flow were identified to evaluate whether these conditions inherently have similar gas holdup radial profiles. Two sets of such conditions extracted from the CREL database are reported here.

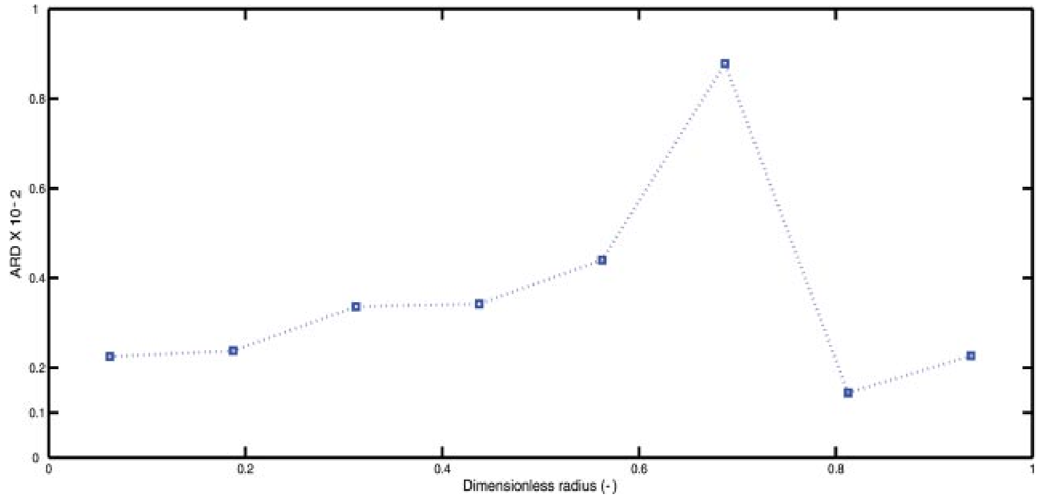

Figure 13. Variation of ARD in liquid axial velocities between similarity conditions (D6P4U30water and D6P4U16 C9–C11) along the column radius in a 0.162 m diameter stainless steel column.

Figure 18 shows a set of experimental conditions with an overall gas holdup close to 0.1. One condition is at 2 cm/s and 0.1 MPa in an air–water system (Ong, 2003), while other one is at 3 cm/s and 0.1 MPa in an air–Therminol LT system (Shaikh and Al-Dahhan, 2005). Based on overall gas holdup studies performed in the respective studies, it is clear that both these conditions are in bubbly flow. The gas holdup radial profiles were close to each other, with AARD of 6%. Figure 19 shows another set of conditions operating in the bubbly flow regime with an overall gas holdup of 0.22. In this set, one conditions is at 5 cm/s and 0.4 MPa in an air–Therminol LT system (Shaikh and Al-Dahhan, 2005), while other one is at 3.5 cm/s and 1 MPa in an air–Therminol LT system (Shaikh, 2007). The gas holdup radial profiles at these conditions were found to be close, with an AARD of 4.5%. These results show that when both operating conditions fall in bubbly flow, the similarity of overall gas holdup *necessarily* results in similar gas holdup radial profiles. As shown in sets of similarity conditions above, such close gas holdup radial profiles would inherently result in similar liquid recirculation and mixing intensity. From

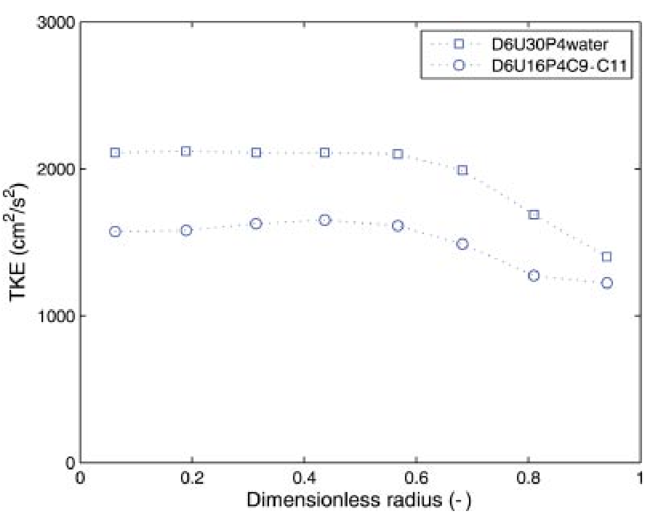

Figure 14. TKE radial profile in a 0.162 m diameter stainless steel column (D6P4U30water: 6 in. diameter column, 0.4 MPa, and 30 cm/s, an air–water; D6P4U16 C9–C11: 6 in. diameter column, 0.4 MPa, and 16 cm/s, air–C9–C11) (overall gas holdup ~0.35).

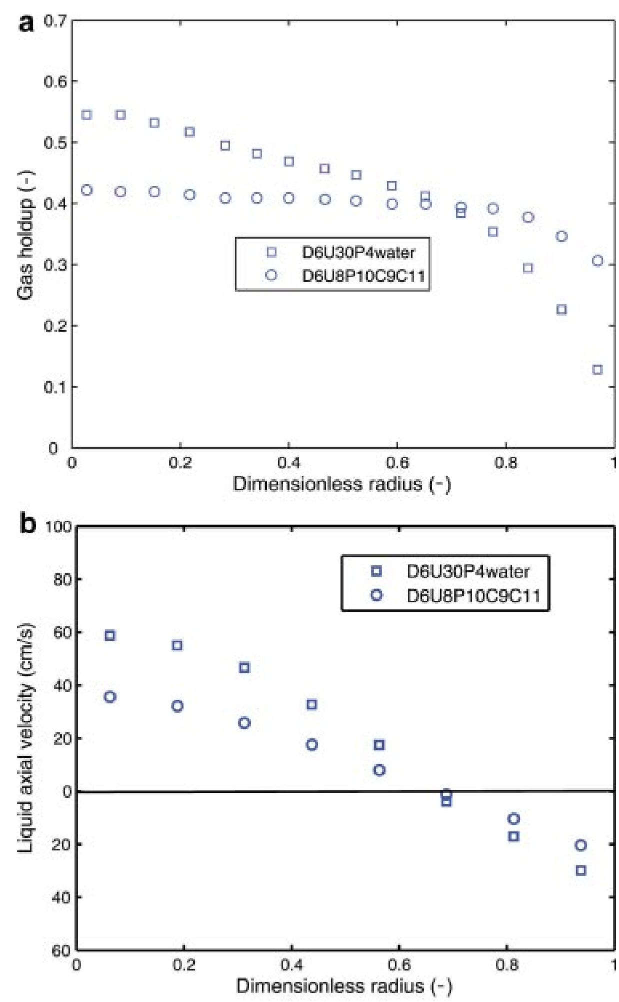

Figure 15. (a) Gas holdup and (b) axial liquid velocity radial profile in a 0.162 m diameter stainless steel column (D6P4U30water: 6 in. diameter column, 0.4 MPa, and 30 cm/s, an air–water; D6P10U8 C9–C11: 6 in. diameter column, 1 MPa, and 8 cm/s, air–C9–C11) (overall gas holdup ~0.35).

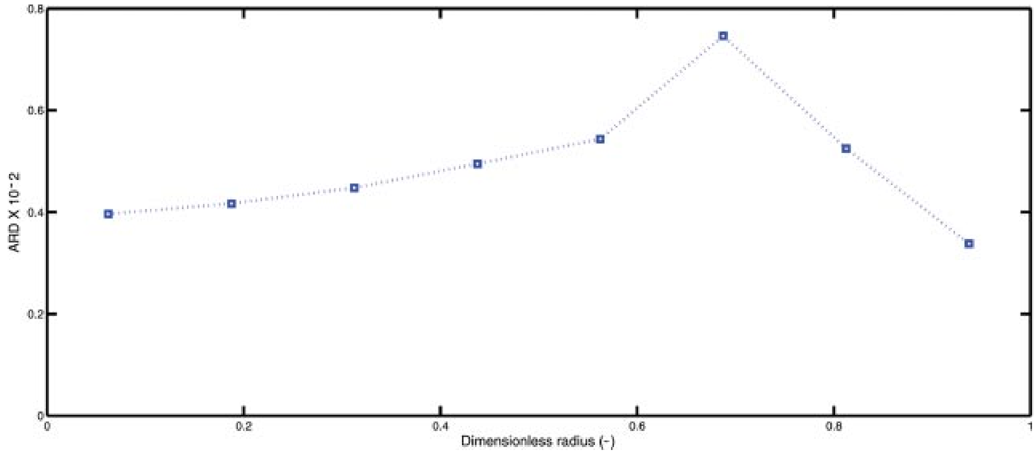

Figure 16. Variation of ARD in liquid axial velocities between similarity conditions (D6P4U30water and D6P10U8 C9–C11) along the column radius in a 0.162 m diameter stainless steel column.

the above comparisons, it is evident that similarity based on global parameters can be generalised *only* when both the conditions are in bubbly flow, because the magnitude of macroscopic hydrodynamics is the controlling hydrodynamic parameter in the presence of uniform holdup distribution across the column cross-section.

The current work cautions against the generalisation of similarity criteria based only on global parameter. It was demonstrated that similarity of global parameters does not necessarily ensure similar hydrodynamic performance, particularly in the churn-turbulent flow regime. The similarity of gas holdup and its distribution along the cross-section or its radial profile are pertinent in obtaining similar recirculation and mixing intensity in two systems.

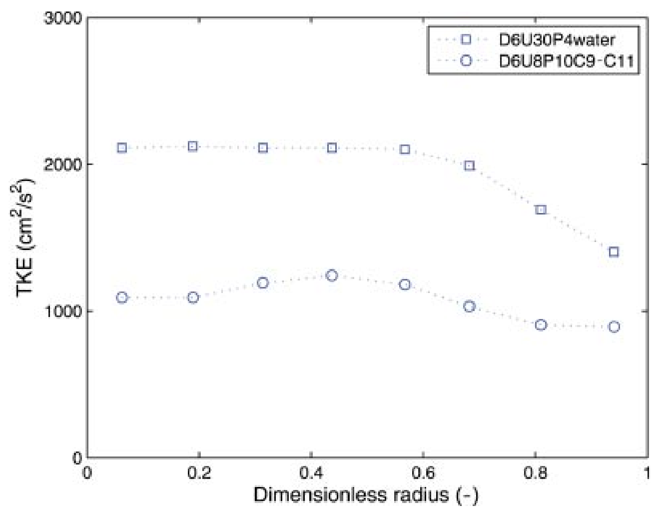

Figure 17. TKE radial profile in a 0.162 m diameter stainless steel column (D6P4U30water: 6 in. diameter column, 0.4 MPa, and 30 cm/s, an air–water; D6P10U8 C9–C11: 6 in. diameter column, 1 MPa, and 8 cm/s, air–C9–C11) (overall gas holdup ~0.35).

EVALUATION OF THE LITERATURE REPORTED DIMENSIONLESS NUMBERS

The objective of this part is to evaluate the commonly proposed dimensionless numbers in literature for scale-up of bubble columns as well as in the correlations of hydrodynamic parameters at the similarity conditions. Since these conditions have the similar magnitude of hydrodynamic and turbulent parameters, it is expected that a set of dimensionless groups will exhibit consistent similarity. Dimensionless numbers used for evaluation are:

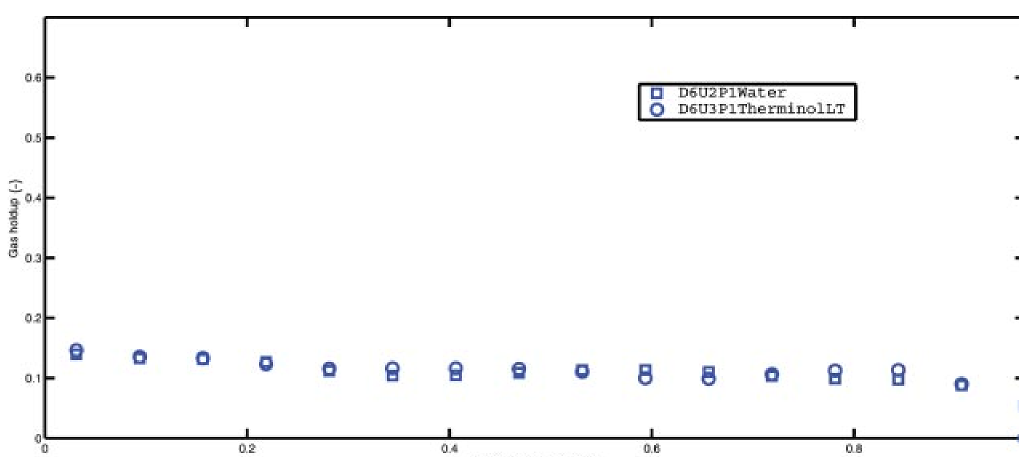

Figure 18. Gas holdup radial profile in a 0.162 m diameter stainless steel column (D6U2P1water: 0.1 MPa and 2 cm/s, an air–water; D6U3P1Therminol LT: 0.1 MPa and 3 cm/s, air–Therminol LT) (overall gas holdup ~0.1).

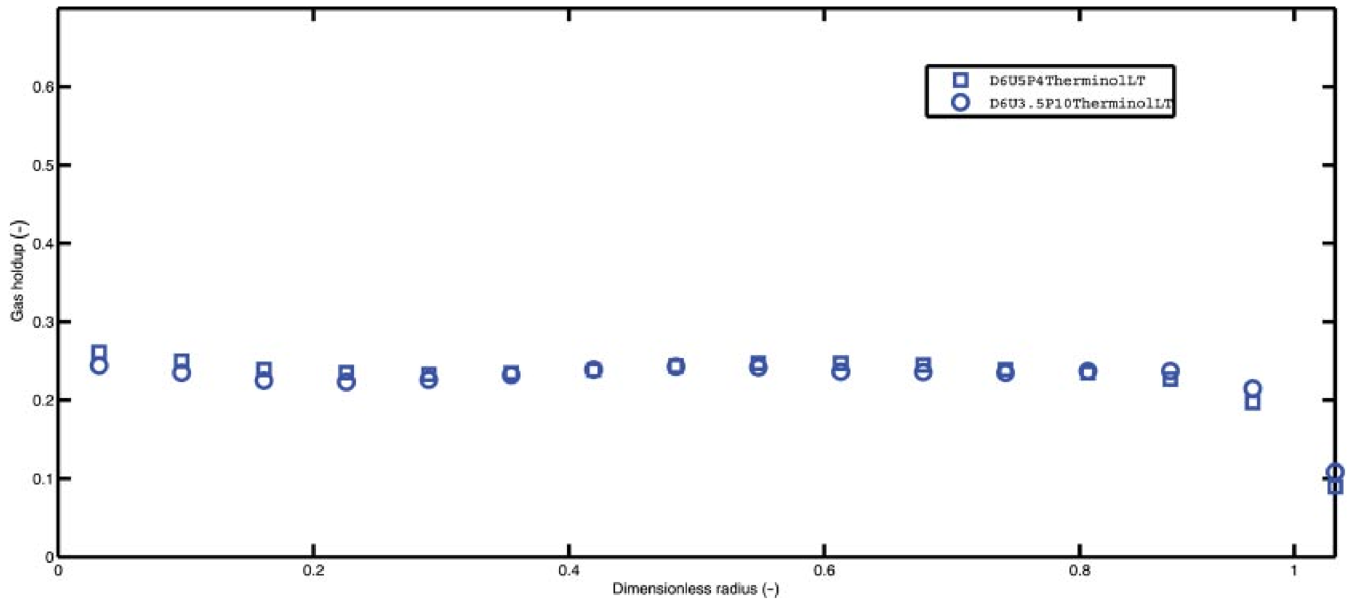

Figure 19. Gas holdup radial profile in a 0.162 m diameter stainless steel column (D6U5P4Therminol LT: 0.4 MPa and 5 cm/s, air–Therminol LT; D6U3.5P10Therminol: 1 MPa and 3.5 cm/s, air–Therminol LT) (overall gas holdup ~0.22).

Morton number, *Mo*; Eotvos number, *Eo*; Reynolds number, *Re*; Density ratio, D_r; Froude number, *Fr*; Weber number, *We*; Bond number, *Ga*; Aspect ratio, L/D. In addition, a dimensionless group proposed by Fan et al. (1999) which is denoted as D was also evaluated. It should be noted that no conscious attempt was made to maintain any of the dimensionless numbers similar during experimental studies, which is clear from the earlier section.

Table 4 shows the comparison of these dimensionless groups for three sets of similarity conditions. An absolute relative difference (ARD) between the conditions of the same set was calculated as defined in Equation (6b).

In the set S1 of similarity conditions, the values of *Eo* and *Ga* are the same. These groups are comprised of liquid physical properties and column diameter. The experimental conditions in this set used the same liquid in the same column at different pressures and superficial gas velocities. Neither pressure nor superficial gas velocity has any effect on liquid physical properties and hence the similarity of these two numbers. In addition, ARD between Morton numbers at these two conditions is close to 4%. This difference is due to the differences in gas density. All remaining dimensionless groups differ by at least 30% of ARD.

In the set S2, the values of *Eo* and *Ga* are the same for the reasons explained above. ARD between Morton numbers in this set is close to 7%. The relatively larger difference in this case is due to larger difference in gas density in the set S2 compared to the set S1. Apart from this, the dimensionless group denoted as D shows ARD of 10%. All remaining dimensionless group exhibit ARD of at least 50%.

The conditions of set S3 have different liquid physical properties at different pressures and the same superficial gas velocity. Hence this set does not show any similarity between *Eo* and *Mo*. ARDs for *Eo* and *Mo* for this set are 150% and 1910%. It shows ARD for *Ga* around 12% while ARD for D around 22%. This set shows only one number the same at both the conditions, that is, *Fr*. All remaining groups exhibit ARD of at least 60%.

In the summary, the first two sets showed the same *Eo* and *Mo* while set S3 showed magnitude of differences in these groups. Group D showed ARD of 10% and 22% in set S2 and S3, respectively. However, it showed 78% of ARD in the set S1. It appears that *Ga* was the only group which was within 15% in all the sets. Set S3 showed the same values of *Fr* number, however, ARDs for *Fr* in set S1 and S2 are 56% and 125%, respectively. Based on above discussion, for available experimental results that show similar hydrodynamics and turbulent parameters, no set of dimensionless groups appear consistently similar to provide any substantial conclusion. Hence, the application and limitations of currently proposed dimensionless groups for hydrodynamic similarity need to be further investigated in detail.

Table 4. Dimensionless groups at similarity conditions

Set	System	Pressure (MPa)	U_g (cm/s)	*Mo*	*Eo*	*Re*	D_r	*Fr*	*We*	*Ga*	D
S1	Air–water	0.1	45	2.62e − 11	3542	7.25e4	0.0012	0.13	453	4.1e10	0.34
	Air–water	0.4	30	2.61e − 11	3542	4.84e4	0.0048	0.057	201	4.1e10	0.61
S2	Air–water	1.0	30	2.59e − 11	3542	4.84e4	0.012	0.057	201	4.1e10	1.53
	Air–water	0.4	45	2.61e − 11	3542	7.25e4	0.0048	0.13	453	4.1e10	1.38
S3	Air–water	0.4	30	2.61e − 11	3542	4.84e4	0.0048	0.057	201	4.1e10	0.61
	Air–C9–C11	0.1	30	5.27e − 10	8846	4.54e4	0.0015	0.057	503	3.6e10	0.48

$Mo = \frac{g(\rho_L-\rho_G)\mu_L^4}{\rho_L^2\sigma_L^3}$; $Eo = \frac{g\rho_L d^2}{\sigma_L}$; $\mathrm{Re} = \frac{dU_g(\rho_L-\rho_G)}{\mu_L}$; $D_r = \frac{\rho_G}{\rho_L}$; $Fr_g = \frac{u_g^2}{gd}$; $We = \frac{\rho_L U_g^2 d}{\sigma_L}$; $Ga = \frac{g\rho_L^2 d^3}{\mu_L^2}$; $D = \frac{U_g^4\rho_G}{\sigma_L g}$

DEVELOPMENT OF METHODOLOGY

In a nutshell, this work has proposed and successfully evaluated a hypothesis for hydrodynamic similarity utilising CT and CARPT. However, to facilitate the proposed methodology for scale-up/scale-down purposes, it needs modelling tools for "a priori" prediction of the needed hydrodynamic parameters. The development of such detailed approach is out of the scope of the current manuscript. However, we wish to outline briefly how we envision developing such method.

An ideal choice for such a task would be fundamentally based computational fluid dynamics (CFD) models and can be used to search the similarity conditions in two reactors. However, searching such conditions using CFD is a time-consuming task. Hence, we propose to develop state-of-the-art correlations for "a priori" prediction of the needed hydrodynamic parameters to search similarity conditions in two reactors.

Towards this goal, the specific focus was to develop unified artificial neural network (ANN) based correlations for overall gas holdup, radial profile of gas holdup, and liquid axial velocity in bubble columns. These correlations were derived from the experimental data bank collected from the open literature that covers wide range of operating and design parameters. Correlations for the following hydrodynamic parameters were developed:

(i) Overall gas holdup (Shaikh and Al-Dahhan, 2003).
(ii) Gas holdup radial profile (Shaikh, 2007).
(iii) Liquid axial velocity radial profile (Shaikh, 2007).
(iv) Centre-line liquid velocity (Shaikh, 2007).

Once the conditions of similarity were identified using these correlations, experimentally validated CFD can be used for further evaluation of design and scale-up. This work will subsequently be published in future manuscripts.

CONCLUSIONS

A new hypothesis for hydrodynamic similarity and subsequently for scale-up of bubble column reactors was proposed and validated. The developed methodology requires the similarity of overall gas holdup as well as of gas holdup radial profile. It was evaluated using single source γ-ray CT and CARPT. The conditions of similarity where overall gas holdup and radial gas holdup profiles were the same, and mismatch where overall gas holdup was the same but gas holdup radial profiles were different, have been identified. The combination of similarity and mismatch experiments showed the importance of maintaining the gas holdup radial profiles the same, not just the overall gas holdup. Such similarity exhibited the similar liquid circulation and mixing intensity in two systems.

This work also showed that the condition that two systems must operate in the same flow regime to be hydrodynamically similar is *necessary* but not *sufficient*. It showed the importance of matching gas holdup radial profiles or cross-sectional distributions in two systems, even if both the systems operate in the same flow regime. Hence, the traditionally used criterion for hydrodynamic similarity, based only on global parameters, can be fatal and needs to be exercised with prudence.

In addition, dimensionless groups reported for hydrodynamic similarity were evaluated for available sets of similarity conditions. It appears that within the range of studied experimental conditions, no consistent set of dimensionless group exhibit similarity. Hence the application and limitations of dimensionless approach for bubble column reactors need to be investigated in detail.

The evaluation of the demonstrated methodology will be further extended to study its utility in different column diameters. It also provides an opportunity to extend it to other multiphase reactor configurations.

NOMENCLATURE

A	absorbance
C_D	drag coefficient
d_b	bubble diameter (m)
D_{zz}	axial turbulent eddy diffusivity
D_{rr}	radial turbulent eddy diffusivity
d	column diameter (cm)
D	dimensionless group proposed by Fan et al. (1999)
Eo	Eotvos number
Fr	Froude number
Ga	Galilei number
I, I_0	intensity of radiation received by detector and emitted by the source
$k_L a$	volumetric mass transfer coefficient (s^{-1})
k_0	first order kinetic constant
L	height of reactor (m)
Mo	Morton number
r/R	dimensionless radius
R_K	relative volumetric coefficient (Equation 3)
Re	Reynolds number
U_g	superficial gas velocity ($cm\,s^{-1}$)
V_b	bubble rise velocity ($m\,s^{-1}$)
V_{b0}	rise velocity of bubble swarms at low superficial gas velocity ($m\,s^{-1}$)
We	Weber number
z	axial location

Greek Letters

ε_G	gas hold up
$\bar{\varepsilon}_G$	cross-sectionally averaged gas holdup
$\rho\mu$	volumetric attenuation coefficient
ρ_L	liquid density ($kg\,m^{-3}$)
β	dimensionless parameter

Subscripts

G	gas
L	liquid
ij	pixel

ACKNOWLEDGEMENTS

The authors are thankful to the High-Pressure Slurry Bubble Column Reactor (HPSBCR) Consortium [Sasol (South Africa), Statoil (Norway), ConocoPhillips (USA), and EniTech (Italy)] and UCR-DOE (DE-FG-26-99FT40594) grants that made this work possible.

REFERENCES

Degaleesan, S., "Fluid Dynamic Measurements and Modeling of Liquid Mixing in Bubble Columns," D.Sc. Thesis, Washington University, St. Louis, MO (1997).
Fan, L.-S., "Gas-Liquid-Solid Fluidization Engineering," Butterworth Series in Chemical Engineering, Boston, MA (1989).

Fan, L.-S., G. Q. Yang, D. J. Lee, K. Tsuchiya and X. Luo, "Some Aspects of High-Pressure Phenomena of Bubbles in Liquids and Liquid-Solid Suspensions," Chem. Eng. Sci. **54**, 4681 (1999).
Han, L., "Hydrodynamics and Mass Transfer in Bubble Column Reactors," D.Sc. Thesis, Washington University, St. Louis, MO (2007).
Inga, J. R. and B. I. Morsi, "Effect of Catalyst Loading on Gas/Liquid Mass Transfer in a Slurry Reactor: A Statistical Experimental Approach," Can. J. Chem. Eng. **75(5)**, 872–881 (1997).
Kemoun, A., B. Cheng Ong, P. Gupta, M. H. Al-Dahhan and M. P. Dudukovic, "Gas Holdup in Bubble Columns at Elevated Pressure Via Computed Tomography," Intl. J. Mult. Flow **27**, 929–946 (2001).
Krishna, R., J. W. A. de Swart, J. Ellenberger, G. B. Martina and C. Maretto, "Gas Holdup in Slurry Bubble Columns: Effect of Column Diameter and Slurry Concentrations," AIChE J. **43**, 311–316 (1997).
Krishna, R., J. M. van Baten, M. I. Urseanu and J. Ellenberger, "Design and Scale-Up of the Bubble Column Slurry Reactor for Fischer-Tropsch Synthesis," Chem. Eng. Sci. **56**, 537–545 (2001).
Kumar, S. B., "Computed Tomography Measurements of Void Fraction and Modeling of the Flow in Bubble Columns," Ph.D. Thesis, Florida Atlantic University, Boca Raton (1994).
Macchi, A., H. Bi, J. R. Grace, C. A. McKnight and L. Hackman, "Dimensional Hydrodynamic Similitude in Three-Phase Fluidized Beds," Chem. Eng. Sci. **56**, 6039–6045 (2001).
Ong, B. C., "Experimental Investigations of Bubble Column Hydrodynamics—Effect of Elevated Pressure and Superficial Gas Velocity," D.Sc. Thesis, Washington University, St. Louis, MO (2003).
Rados, N., "Slurry Bubble Column Hydrodynamics," D.Sc. Thesis, Washington University, St. Louis, MO (2003).
Safoniuk, M., J. R. Grace, L. Hackman and C. A. McKnight, "Use of Dimensional Similitude for Scale-Up of Hydrodynamics in Three-Phase Fluidized Bed," Chem. Eng. Sci. **54**, 4961–4966 (1999).
Shaikh, A., "Bubble and Slurry Bubble Columns: Mixing, Flow Regime Transition, and Scaleup," D.Sc. Thesis, Washington University, St. Louis, MO (2007).
Shaikh A. and M. H. Al-Dahhan, "Development of an Artificial Neural Network Correlation for Prediction of Overall Gas Holdup in Bubble Column Reactors," Chem. Eng. Proc. **42**, 599–610 (Special Issue on Application of Neural Networks to Multiphase Reactors) (2003).
Shaikh, A. and M. Al-Dahhan, "Characterization of the Hydrodynamic Flow Regime in Bubble Columns via Computed Tomography," Flow Meas. Instrum. **16**(2–3), 91–98 (Special Issue on Tomographic Techniques for Multiphase Flow Measurements) (2005).
Shaikh, A. and M. Al-Dahhan, "A Review on Flow Regime Transition in Bubble Columns," Intl. J. Chem. React. Eng. **5**, R1 www.bepress.com/ijcre/vol5/R1 (2007).
van Baten, J. M., J. Ellenberger and R. Krishna, "Scale-Up Strategy for Bubble Column Slurry Reactors Using CFD Simulations," Cat. Today **79–80**, 259–265 (2003).
Wilkinson, P. M., A. P. Spek and L. L. van Dierendonck, "Design Parameters Estimation for Scale-Up of High Pressure Bubble Columns," AIChE J. **38**(544), (1992).
Zhang, K. and Y. Zhao, "A Scale-Up Strategy for Low-Temperature Methanol Synthesis in a Circulating Slurry Bubble Reactor," Chem. Eng. Sci. **61**, 1459–1469 (2006).

Manuscript received December 4, 2009; revised manuscript received March 26, 2010; accepted for publication March 29, 2010.